JSR Publications

Available Online

J. Sci. Res. **15** (3), 595-605 (2023)

JOURNAL OF SCIENTIFIC RESEARCH

www.banglajol.info/index.php/JSR

Mitigation of Edge Ringing for the Optimization of Highly Aberrated Coherent Optical Systems

P. Shailaja[1*], S. V. Rao[1], D. K. Sagar[2], M. Venkanna[3]

[1]Department of Physics, Jawaharlal Nehru Technological University, Hyderabad, India

[2]Optics Research Group, Department of Physics, Osmania University, Hyderabad, India

[3]Department of Physics, BVRIT Hyderabad College of Engineering for Women, Hyderabad, India

Received 29 November 2022, accepted in final revised form 13 May 2023

Abstract

The images of straight-edge objects formed by a coherent optical system with a circular aperture apodized with a shaded aperture have been studied. Image quality assessment parameters such as edge-ringing, edge-gradient, and edge-shift of the edge fringes have been investigated as a function of apodization parameters for various degrees of defocus, coma, and primary spherical aberrations. The reduction in the ringing pattern is more effective at the suitable combination of aberrations than the aberration-free cases and attains the minimum value for φ_s=2π where it is completely balanced with φ_d. It has been found that the image quality of straight-edge objects can be improved by combining specific aberrations with the appropriate apodizer.

Keywords: Amplitude filters; Apodization; Aberrations; Edge-ringing; Optical systems.

doi: http://doi.org/10.3329/jsr.v15i3.63023 J. Sci. Res. **15** (3), 595-605 (2023)

1. Introduction

The existence of optical aberrations is a ubiquitous feature of all optical systems. Even the best-corrected systems have residual aberrations, and most systems are not well-corrected. As the wavefront travels through the optical systems, aberrations cause phase problems. Aberrations can lead to unfavorable outcomes and a decrease in optical system performance. In an aberrated optical system, edge ringing and shifting are more prominent than in an aberration-free one. Apodized images of coherently illuminated edges in the presence of aberrations were examined in depth [1]. Marechal has studied the best balancing conditions for a coherently lighted line in the presence of spherical aberration and defocusing [2].

Apodization is the deliberate modification of the transmittance of an optical system, which affects the imaging characteristics of the optical system. The exploit of apodization is useful in controlling the effects of aberrations in coherent systems. Defocus is the simplest sort of aberration in that; the real wavefront differs from the spherical reference

*Corresponding author: shailajakiran2007@gmail.com

wavefront simply in its radius of curvature. A radially symmetric aberration is a spherical aberration. It refers to the wavefront that deviates the most from the spherical reference wavefront of all the aberrations considered. The incident wavefront is tilted or decentered with respect to the optical surface, which causes coma aberration. As a result, it's either an aberration affecting off-axis picture spots or an axial misalignment of optical surfaces. Edge ringing, edge gradient, and edge shifting are three significant effects that impair the image in coherent imaging of edge objects. The results of experiments on the impact of defocusing, coma, and primary spherical aberrations on the performance of apodized coherent optical imaging systems in forming straight-edge images are reported in this work.

When the prerequisites of linearity are met, Fourier analytical methods can be applied to optical systems with space invariance and unit magnification. The picture of a one-dimensional edge object lit coherently is obtained at the image plane using Fourier techniques and an image generation system. When the system is linear in object and image amplitudes with the pupil function linking them, coherent lighting can be considered a linear image-generating system. The final image intensity distribution is the consequence of the sum of the complex amplitudes to form the complex amplitude distributions with its squared modulus. In the instance of coherent illumination, the Edge response, which is the core mathematical model, was generated by applying the coherent image generation scheme utilizing Fourier analytical methods. The response of the optical system with a generalized shaded aperture has been investigated for various apodization parameter values.

Apodization can be achieved in a number of methods, including changing the aperture's geometry or transmission qualities [3]. The former is referred to as aperture shaping, and it involves changing the shape and size of the aperture. Secondly, an apodized filter over the pupil is known as aperture shading. Thus, apodization is the deliberate manipulation of the pupil function to change the light distribution in the PSF to improve image quality [4]. In optics, apodization is comparable to pulse shaping in electrical engineering [5,6]. Straubel is credited as being the inventor of the apodization theory [7]. The higher spatial frequencies are reduced as the amplitude transmittance of the pupil is gradually reduced from the center to the edge of the pupil, resulting in the suppression of side lobes. Apodization is a subset of the more general spatial filtering approach [3]. Apodization can help an aberrated optical system improve certain aspects of its imaging performance [8-10]. To improve image quality, some researchers have investigated various pupil functions' edge-ringing and edge-shifting aspects [11-13]. The difference between the first maximum of the edge fringes and the unit object intensity is the edge ringing. Edgeshift, also known as image shift, is the distance between the image edge and half of the object edge's intensity value. The rise in image intensity over a unit change in Z around the geometric edge (i.e., Z=0) is known as an edgegradient. Building a system that produces actual and positive amplitude impulses is desirable to avoid edge-ringing in coherent and partially coherent illuminations. This problem has been investigated, and determined that a proper apodizer can control edge-ringing [14-16]. In

the absence and presence of aberrations, aperture shaping reduces the negative effects of edge-ringing incoherent images. The appearance of a sharp cut-off in the transfer function distinguishes a coherent optical system. The high-frequency components of an edge object are quite powerful. Compared to the sharp edge's Fourier spectrum, the coherent optical system's cut-off is effectively low, resulting in undesirable edge ringing [17].

Apodization can be employed for a variety of objectives, including suppressing optical side-lobes in the diffraction field of optical imaging systems [18-19], enhancing the depth of field [20-24], and improving the resolution [25-30]. The effectiveness of the apodization technique is always connected to the design of pupil function. It is well known that apodization, which is used to lower the size of the point spread function's focus spot, frequently results in the growth of side lobes. As a result, many techniques for reaching a compromise are examined [31-35].

2. Theory and Formulation

The mathematical expression of amplitude transmittance of an opaque straight-edge object [36] is given by

$B(u, v) = 1$ when $u \geq 0$

$B(u, v) = 0$ when $u < 0$ (1)

It is evident that B (u) is a non-convergent and does not permit Fourier transformation directly. However, this difficulty can be overcome by expressing it in terms of the "signum" function as

$$B(u) = \frac{1}{2}\left[1 + Sgn(u)\right]$$

Where $Sgn(u)$ is expressed as

$Sgn(u)$ =1 when $u \geq 0$

= -1 when $u <0$ (2)

Any transformable function which approaches $Sgn(u)$ should be considered, as this function also has a discontinuity at u=0.

For example, the function

$$f(u) = [exp(-\sigma|u|)\, Sgn(u)] \rightarrow Sgn(u) as \sigma \rightarrow 0 \quad (3)$$

Hence the Fourier transform of equation (3) will be

$$F.T.[f(u)] = \int_{-\infty}^{\infty} exp(-\sigma|u|)\, Sgn(u)\, exp(-2i\pi ux)\, du$$

$$= \int_{-\infty}^{0} -exp[(\sigma - i2\pi x)u]\, du + \int_{0}^{\infty} exp[(-\sigma + i2\pi x)u]\, du$$

$$= -\frac{1}{(\sigma - i2\pi x)} + \frac{1}{(\sigma + i2\pi x)} \quad (4)$$

As $\sigma \to 0$, the above expression equals to $\left(\frac{1}{i\pi x}\right)$ i.e.,

$$F.T[f(u)] = exp[(-\sigma|u|)Sgn(u)] = \frac{1}{i\pi x}$$

Thus expressing the straight edge in terms of $Sgn(u)$ as given in (2), and its Fourier transform can be obtained as

$$F.T.[B(u,v)] = F.T.\left[\frac{1}{2}\{1 + Sgn(u)\}\right]$$

$$= \int_{-\infty}^{\infty} \left[1 + \left(-\sigma|u|Sgn(u)\right)\right] exp(-i2\pi ux)\, dx$$

$$= \tfrac{1}{2}\left[\delta(x) + \tfrac{1}{i\pi x}\right] \quad (5)$$

Here, $\delta(x)$ is the well–known Dirac-delta function. The expression (5) represents the Fourier spectrum of the object amplitude distribution. In this spectrum, the presence of a large zero frequency component at $x = 0$ is observed, in addition to other non-zero frequency components. Looking at the object function in figure1, it appears at first sight that $B(u,v)$ is purely zero frequency input to the optical system, and therefore, the presence of those non-zero frequencies in the spectrum of such an object may appear rather strange. It should be, however, observed that the objective function has zero transmission over one-half in its own plane and a transmission equal to unity over the other half. In other words, $B(u,v)$ is zero for $u< 0$ and then there is an abrupt discontinuity at$u = 0$. Thus, $B(u,v)$ is not a true D.C. signal as it is not constant over the entire interval ranging from$-\infty$ to∞, and this describes the presence of other frequency components in the spectrum.

The imaging positions encountered in optics are generally concerned with objects where amplitude or intensity variations are to be considered in two dimensions. The complex object amplitude distribution, as defined in equation (1), implies that there is no variation in amplitude transmission of the object along the entire y-direction. This will give rise to an infinite impulse at $y = 0$ in the spectrum plane and can be represented by the Dirac-delta function $\delta(y)$. Finally, therefore, the two-dimensional F.T. of the objective function is obtained as

$$a(x,y) = \tfrac{1}{2}\left[\delta(x) + \tfrac{1}{i\pi x}\right]\delta(y) \quad (6)$$

The above expression gives the amplitude distribution spectrum of the object $B(u,v)$ at the entrance pupil of the optical system. The modified amplitude distribution spectrum of the object at the exit pupil of the optical system can be expressed as

$$a'(x,y) = a(x,y).T(x,y) \quad (7)$$

Here $T(x,y)$ represents the pupil function of the given optical system having aberrations and can be expressed as

$$T\ (x,y) = f(x,y)\, exp[\, i\varphi(x,y)] \quad (8)$$

Where f(x, y) denotes the amplitude transmittance over the pupil and φ(x, y) indicates the wave aberration function of the optical system. In the absence of apodization, f(x, y) is taken to be equal to unity, i.e., for the Airy pupils, f(x, y) = 1.

For defocus, coma, and primary spherical aberrations, the aberration function can be expressed as

$$r \quad = \sqrt{x^2 + y^2}\varphi\ (x,y) = \left[- \left(\frac{1}{2}\varphi_d r^2 + \frac{1}{3}\varphi_c Cos(\theta) r^3 + \frac{1}{4}\varphi_s r^4 \right) \right] \rightleftarrows$$

Here φ_d-Defocus coefficient, φ_s-Primary spherical aberration coefficient and φ_C - Coma and

From the expressions (6), (7), and (8), the modified amplitude spectrum at the exit pupil is given by

$$a'(x,y) = \frac{1}{2}\left[\delta(x) + \frac{1}{i\pi x}\right] \delta(y) f(x,y)\, exp[\, i\varphi(x,y)] \tag{9}$$

The above equation (9) gives the object's modified spectrum at the optical system's exit pupil. The inverse Fourier Transform of expression will give the amplitude distribution spectrum in the image plane (9). Therefore,

$$B'(u',v') = \frac{1}{2}\int_{-\infty}\int^{+\infty} \left[\delta(x) + \frac{1}{i\pi x}\right] \delta(y) f(x,y)\, exp[i\varphi(x,y)]$$

$$exp[\rightleftarrows 2 \rightleftarrows \pi \rightleftarrows\rightleftarrows\rightleftarrows\rightleftarrows i(u'x + v'y)]\, dxdy \tag{10}$$

The integration limits of equation (10) are only formal because the pupil function given by T(x, y) vanishes outside the pupil and can be assumed to be unity inside. Thus, after some manipulation in the integration of Eq. (10) by employing the filtering property of the Dirac-delta function, the expression (10) can be simplified as

$$B'(u',v') = \frac{1}{2} f(0,0)\, exp(\, i\varphi(0,0)) + \frac{1}{2\pi}\int_{-1}^{1} f\,(x,0) \frac{cos(\varphi(x,0) + 2\pi u'x)}{x} dx$$

$$-\frac{i}{2\pi}\int_{-1}^{1} f(x,0) \frac{cos(\varphi(x,0)+2\pi u'x)}{x} dx \tag{11}$$

The filtering property of the Dirac-delta function is represented by

$$\int_{-\infty}^{+\infty} \delta(x)\, f(x) dx = f(0) \tag{12}$$

For the central transmittance of the pupil function f(0)=1, then the expression (11) can be expressed as

$$B'(u',v') =$$

$$\frac{1}{2} + \frac{1}{2\pi}\int_{-1}^{1} f(x,0)\, exp[i\varphi(x,0)] \frac{sin(2\pi u'x)}{x} dx -$$

$$\frac{i}{2\pi}\int_{-1}^{1} f(x,0)\, exp[i\varphi(x,0)] \frac{sin(2\pi u'x)}{x} dx \tag{13}$$

For the rotationally symmetric pupil function

$$f(x,y) = f(-x,-y)$$

Setting $2\pi u' = Z$in equation (13), then it reduces to the more explicit formula for the image of an edge object.

$$B'(Z) = \frac{1}{2} + \frac{1}{2\pi}\int_{-1}^{1} f(x,0)\, exp[i\varphi(x,0)]\frac{Sin(Zx)}{x}dx \quad (14)$$

On further simplification, equation (14) reduces to

$$B'(Z) = \frac{1}{2} + \frac{1}{\pi}\int_{0}^{1} f(x,y)\, exp[i\varphi(x,0)]\frac{\{Sin(Zx)\}}{x}dx \quad (15)$$

The present work deals with the 1-D straight-edge object, and hence the general form of amplitude distribution is given by

$$B'(Z) = \frac{1}{2} + \frac{1}{\pi}\int_{0}^{1} f(x,\rightleftarrows 0)\, exp[i\varphi(x,0)]\frac{\{Sin(Zx)\}}{x}dx \quad (16)$$

Pupil function f(r) for the shaded aperture is given by

$$f(r) \quad = 1 - \beta r^2$$

Here β is the apodization parameter that controls the level of non-uniformity of transmission over the pupil. β= 0 corresponds to a diffraction-limited airy pupil with uniform unity transmission.

For the given pupil apodized with a shaded aperture in the presence of defocus, primary spherical aberration, and coma, the expression (16) becomes

$$B'(Z) = \frac{1}{2} + \frac{1}{\pi}\int_{0}^{1} Cos^2(\pi\beta r)\, exp[-i(\varphi_d \frac{x^2}{2} + \frac{1}{3}\varphi_c Cos(\theta) r^3 + \varphi_s \frac{x^4}{4})]\frac{sin(Zx)}{x}dx \quad (17)$$

$$I(Z) = |B'(Z)|^2 \quad (18)$$

The intensity distribution of an edge image formed by an apodizedaberrated optical system is given by the squared modulus of expression (17)

3. Results and Discussion

The impact of defocus, primary spherical aberration, and coma on the images of straight-edge objects produced by coherent optical systems and apodized by the shaded aperture in the case of circular aperture has been studied by employing Matlab simulation and the expression (18). For several values of the dimensionless diffraction variable Z ranging from –3 to 20, the intensity distribution of images of straight-edge objects has been studied. Various degrees of apodization has been explored as a function of image quality evaluation metrics such as edge-ringing, edge-gradient, and edge-shift of the edge fringes.

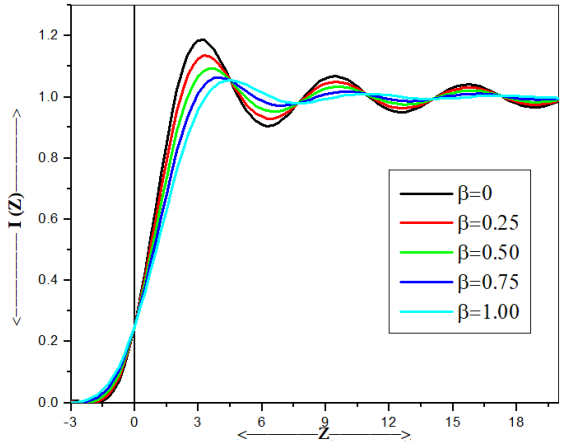

Fig. 1. Image intensity distribution curves for the aberration-free optical system.

Fig. 2 depicts the intensity distribution curves in the case of a circular aperture for an aberration-free optical system. It is clear that the edge-ringing is the maximum in the case of clear aperture (β= 0), i.e., the magnitude of edge-ringing is the highest in the case of unapodized optical systems. The edge-ringing and edgegradient is reduced while increasing of edge shift as β changes from 0 to 1. Figs. 3 and 4 depict the intensity distribution curves in the case of circular aperture in the presence of aberrations such as defocus, coma, and primary spherical aberration, where defocus and coma are kept fixed at φ_d=φ_c=π with θ = 0 for different magnitudes of primary spherical aberration when β is varied from 0 to 1 in steps of 0.25. It is observed that for β = 0.75, there is a maximum control in edge-ringing for the given combination of φ_d=φ_c=π and for the values of φ_s= π and 2π at θ = 0 while the edge-gradient and edge shift attains the maximum and the minimum values, respectively.

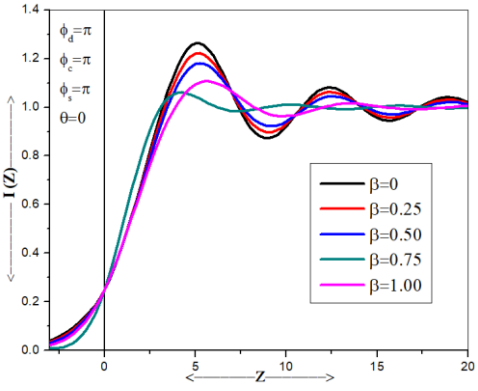

Fig. 2. Image intensity distribution curves for aberrated optical system.

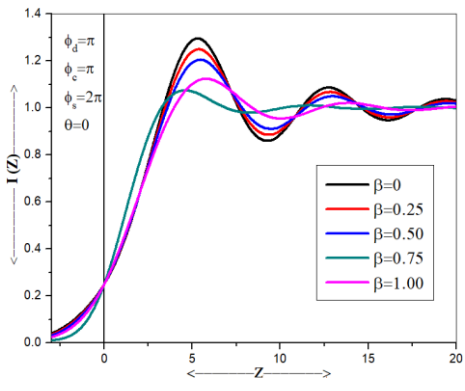

Fig. 3. Image intensity distribution curves for aberrated optical system.

Fig. 4 shows that the edge ringing is decreasing with the apodization parameter β for all values ofφ_s atφ_d=φ_c=π. And it is also observed that for a given β value, the ringing increases with φ_s. The edge ringing is the maximum at φ_s=2π for β=0, i.e., 0.2967, and it is the minimum at φ_s=0 for β=1, i.e., 0.0872. It means the edge ringing can be minimized by the operation of apodization, even in the presence of aberrations. The edge ringing attains the minimum values at β=1 for all values of φ_s=0, π/2, π, 3π/2 and 2π respectively, at the cost of decrease of edge gradient and increase of edge shift.

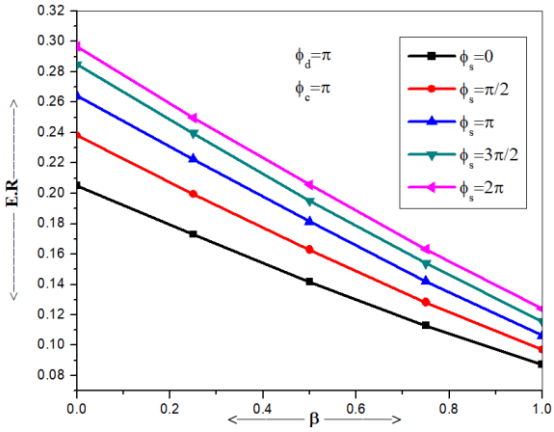

Fig. 4. Variation of edge-ringing with β.

Fig. 5 shows the variation of edge gradient with the apodization parameter β for a given value of φ_d =φ_c=π. For φ_s=0, the edge gradient is gradually decreasing as β varies from 0 to 1. For φ_s= π/2, π, 3π/2 and 2π edge gradient shows an increasing trend from β=0 to 0.75, however, it is decreasing for β>0.75. It is the minimum atβ=0 for φ_s=2π, i.e., 0.1258, and is the maximum at β=0.75 for φ_s=π/2, i.e., 0.2279.

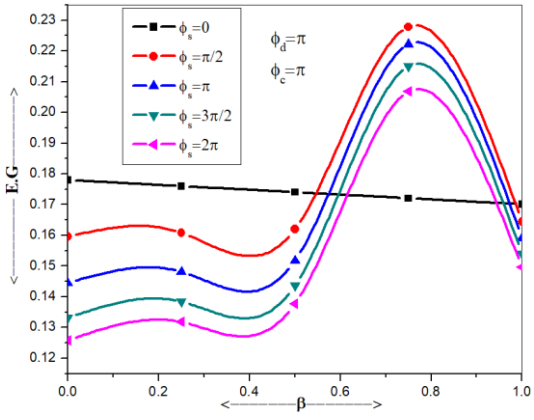

Fig. 5. Variation of edge-gradient with β.

Fig. 6 shows the variation of edge shift with apodization parameter β for a given value of φ_d=φ_c=π. For φ_s=0, the edge shift is increasing as β varies from 0 to 1. For φ_s= π/2, π, 3π/2 and 2π edge shift shows oscillatory changes. However, it attains the minimum values at β=0.75. The shift is the maximum at β=0 for ϕ_s=2π, i.e., 1.4950, and is the minimum at β=0.75 for ϕ_s=π/2, i.e., 0.8850.

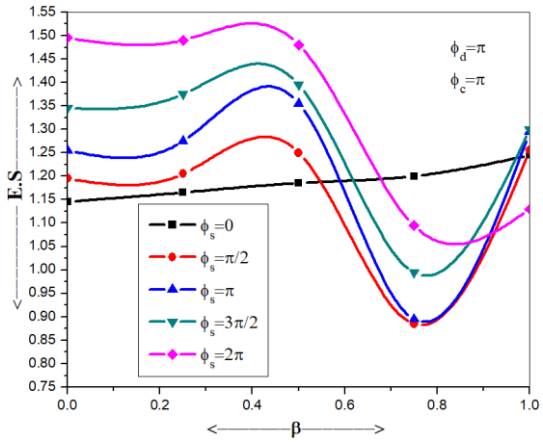

Fig. 6. Variation of edge-shift with β.

Conclusion

Apodization of the given optical system by the shaded optical filter mitigates the deleterious effect of the edge ringing in the presence of aberrations. The image intensity distribution at the straight edge rises monotonically from the dark to bright regions. The edge-ringing increases with coma as it increases from φ_c=0 to π, for β = 0.25. But the pronounced ringing due to the presence of coma has been mitigated gradually at certain defocused planes such as φ_d= π/2, π, 3π/2 and 2π when θ = π. The edge imaging characteristics of the optical system improved when the optical system was apodized with β = 0.75. The elimination of ringing is achieved with minimum edgeshift, and there is a considerable improvement in edge-gradient for certain combinations of aberrations at β=0.75. The reduction in the ringing pattern is more effective at the suitable combination of aberrations than the aberration-free cases and attains the minimum value for φ_s=2π where it is completely balanced with φ_d. Thus, the degraded edge imaging characteristics due to one type of aberration has been recompensed by introducing some other type of aberrations.

References

1. R. Barakat, J. Opt. Soc. Am. **59**, 1432 (1969). https://doi.org/10.1364/JOSA.59.001432
2. M. Born and E. Wolf, Principles of Optics, 7th Edition (Cambridge University press, 1999).
3. E. Hecht andA.Zajac, Optics, 2nd Edition (Addison – Wesley, USA, 1987) pp.422, 496, 497, 512.

4. W. B. Wetherell, R. R. Shannon,and J. C. Wyan, Ed. Ch.6 (Academic Press, 1980) Vol. **8**, pp.173-283.
5. A. Papoulis, J. Opt. Soc. Am. **57**, 362 (1967).https://doi.org/10.1364/JOSA.57.000362
6. A. Papoulis, Systems and Transforms with Applications in Optics (McGraw-Hill, USA, 1968) pp. 442.
7. K. P. Rao, P. K. Mondal, and T. S. Rao, Optic **50**, 73 (1978).
8. R. Barakat, J. Opt. Soc. Am. **52**, 264 (1962).https://doi.org/10.1364/JOSA.52.000264
9. M. Venkanna, N. Sabitha, and D. K. Sagar, J. Sci. Res. **15**, 121 (2023). https://doi.org/10.3329/jsr.v15i1.60366
10. M. Venkanna and S. D.Karuna, J. Adv.Optics **2014**, ID 963980 (2014). https://doi.org/10.1155/2014/963980
11. P.K Katti and B.N. Gupta, J. Opt. Soc. Am. **62**, 41 (1972). https://doi.org/10.1364/JOSA.62.000041
12. H. F. A Tschunko, Appl. Optics **18**, 955 (1979). https://doi.org/10.1364/AO.18.000955
13. T.Araki and T. Asakura, Opt. Commun. **20**, 373 (1997). https://doi.org/10.1016/0030-4018(77)90207-3
14. M.Venkannaand S. D. Karuna, Proc. SPIE **2015**, ID 96540A (2015). https://doi.org/10.1117/12.2181610
15. M. Venkanna and S. D. Karuna, Comput. Optics **46**, 388 (2022). https://doi.org/10.18287/2412-6179-CO-940
16. F. G. Leaver and R. W. Smith, Optik **39**, 156 (1973). https://doi.org/10.3817/0673016156
17. P. S. Considine, J. Opt. Soc. Am. **56**, 1001 (1966). https://doi.org/10.1364/JOSA.56.001001
18. P. Jacquinot and B. R. –Dossier **3**,129 (1964). https://doi.org/10.1016/S0079-6638(08)70570-5
19. G. G.Siu, L.Cheng, and D. S. Chiu, J. Phys. D: Appl. Phys. **27**, 459 (1994). https://doi.org/10.1088/0022-3727/27/3/005
20. E. R. Dowski and W. T.Cathey, Appl. Opt. **34**, 1859(1995). https://doi.org/10.1364/AO.34.001859
21. C. Pan, J.Chen, R. Zhang, and S. Zhuang, Opt. Express **16**, ID 13364 (2008). https://doi.org/10.1364/OE.16.013364
22. S. N.Khonina and A. V. Ustinov, Pattern Recog. Image Anal. **25**, 626 (2015). https://doi.org/10.1134/S1054661815040100
23. A.P.Dzyuba, P.G,Serafimovich, S.N.Khonina, and S. B. Popov, Proc. SPIE **11516**, 115161A (2020). https://doi.org/10.1117/12.2565993
24. S. N. Khonina,S. G. Volotovskiy, A. P. Dzyuba, P. G.Serafimovich, S. B.Popov, and M. A.Butt, Electronics (MDPI), **10**, 1327 (2021). https://doi.org/10.3390/electronics10111327
25. R. Barakat, J. Opt. Soc. Am. **52**, 276 (1962). https://doi.org/10.1364/JOSA.52.000276
26. M.Kowalczyk, C. J.Zapata-Rodriguez, and M.Martinez-Corral, Appl. Opt. **37**, 8206 (1998). https://doi.org/10.1364/AO.37.008206
27. S. N. Khonina and A. V.Ustinov, J. Eng.**2013**, ID 512971 (2013). https://doi.org/10.1155/2013/512971
28. A. N. K. Reddy, D. K.Sagar, and S. N. Khonina, Opt.Spectros. **123**, 940 (2017). https://doi.org/10.1134/S0030400X17120189
29. A. N. K.Reddy and S. N.Khonina, Appl. Phys. B **124**, 229 (2018). https://doi.org/10.1007/s00340-018-7101-z
30. A. N. K.Reddy, M.Hashemi, and S. N. Khonina, Pramana – J. Phys. **90**, 77 (2018). https://doi.org/10.1007/s12043-018-1566-5
31. H. H. Hopkins and B. Zalar, J. Mod. Opt. **34**, 371 (1987). https://doi.org/10.1080/09500348714550391
32. C. J. R.Sheppard and A.Choudhury, Appl. Opt. **43**, 4322 (2004). https://doi.org/10.1364/AO.43.004322
33. C. Ratnam, L. V. Rao, and S. L. Goud, J. Phys. D: Appl. Phys. **39**, 4148 (2006). https://doi.org/10.1088/0022-3727/39/19/005

34. S. N. Khonina, A. V.Ustinov, and E. A. Pelevina, J. Opt. **13**, ID 095702 (2011). https://doi.org/10.1088/2040-8978/13/9/095702
35. S. N. Khonina and S. G. Volotovskiy, Adv. Opt. Technol. **2013**, ID 267684 (2013). https://doi.org/10.1155/2013/267684
36. T. Araki and T Asakura, Optika Aplicata,**VIII**/4, 159 (1978).